### Title
Mechanism of Diacylglycerol-induced Membrane Targeting and Activation of Protein Kinase Cδ*




### Journal
Journal of Biological Chemistry, 279(28)

### ISSN
0021-9258



### Authors
Stahelin, Robert V
Digman, Michelle A
Medkova, Martina
et al.



### Publication Date
2004-07-01

### DOI
10.1074/jbc.m403191200

THE JOURNAL OF BIOLOGICAL CHEMISTRY
Vol. 279, No. 28, Issue of July 9, pp. 29501–29512, 2004
Printed in U.S.A.


# Mechanism of Diacylglycerol-induced Membrane Targeting and Activation of Protein Kinase Cδ*

Received for publication, March 22, 2004, and in revised form, April 16, 2004
Published, JBC Papers in Press, April 22, 2004, DOI 10.1074/jbc.M403191200

**Robert V. Stahelin, Michelle A. Digman, Martina Medkova‡, Bharath Ananthanarayanan, John D. Rafter, Heather R. Melowic, and Wonhwa Cho§**

*From the Department of Chemistry, University of Illinois, Chicago, Illinois 60607*

**The regulatory domains of novel protein kinases C (PKC) contain two C1 domains (C1A and C1B), which have been identified as the interaction site for *sn*-1,2-diacylglycerol (DAG) and phorbol ester, and a C2 domain that may be involved in interaction with lipids and/or proteins. Although recent reports have indicated that C1A and C1B domains of conventional PKCs play different roles in their DAG-mediated membrane binding and activation, the individual roles of C1A and C1B domains in the DAG-mediated activation of novel PKCs have not been fully understood. In this study, we determined the roles of C1A and C1B domains of PKCδ by means of *in vitro* lipid binding analyses and cellular protein translocation measurements. Isothermal titration calorimetry and surface plasmon resonance measurements showed that isolated C1A and C1B domains of PKCδ have opposite affinities for DAG and phorbol ester; *i.e.* the C1A domain with high affinity for DAG and the C1B domain with high affinity for phorbol ester. Furthermore, *in vitro* activity and membrane binding analyses of PKCδ mutants showed that the C1A domain is critical for the DAG-induced membrane binding and activation of PKCδ. The studies also indicated that an anionic residue, Glu$^{177}$, in the C1A domain plays a key role in controlling the DAG accessibility of the conformationally restricted C1A domain in a phosphatidylserine-dependent manner. Cell studies with enhanced green fluorescent protein-tagged PKCδ and mutants showed that because of its phosphatidylserine specificity PKCδ preferentially translocated to the plasma membrane under the conditions in which DAG is randomly distributed among intracellular membranes of HEK293 cells. Collectively, these results provide new insight into the differential roles of C1 domains in the DAG-induced membrane activation of PKCδ and the origin of its specific subcellular localization in response to DAG.**

Protein kinase C (PKC)[1] are a family of serine/threonine kinases that mediate a wide variety of cellular processes (1, 2). Molecular cloning has identified more than 10 members of the PKC family. All PKCs contain an amino-terminal regulatory domain and a carboxyl-terminal catalytic domain. Based upon structural differences in the regulatory domain, PKCs are typically subdivided into three classes; conventional PKC (α, βI, βII, and γ subtypes), novel PKC (δ, ε, η, and θ subtypes), and atypical PKC (ζ and λ/ι subtypes). PKCδ is the first novel PKC isoform to be identified (3) and perhaps the most extensively studied one. PKCδ is ubiquitously distributed among mammalian cells and tissues (4, 5), suggesting universal roles in mammals. Whereas PKCδ has been generally implicated in cell growth inhibition (6–8) and apoptosis (9–11), it has been also shown to exert opposite effects in some cells (12). Recent gene disruption studies have also indicated that PKCδ has cell type-specific functions, including negative regulation of proliferation of B cells (13), reduction in antigen-induced degranulation in mast cells (14), and homeostasis of smooth muscle cells (15). In some mammalian cells, PKCδ has been reported to have opposing functions to another novel PKC, PKCε (7, 16–18). Understanding the molecular basis of these cellular functions of PKCδ would require elucidation of the mechanism by which this novel PKC is specifically targeted to the membrane and activated.

It has been reported (19) that cellular PKCδ activities are regulated by phosphorylation, proteolysis, *sn*-1,2-diacylglycerol (DAG), and other lipids. PKCs have three common phosphorylation sites in the activation loop, turn motif, and hydrophobic motif, respectively (20, 21). Phosphorylation on these sites by either upstream protein kinases (22, 23) or autophosphorylation (24) has been proposed to be essential for the full expression of enzyme activities. PKCδ also has activation loop, turn, and hydrophobic motif sites at Thr$^{505}$, Ser$^{643}$, and Ser$^{662}$ (25, 26), respectively, which are substantially phosphorylated *in vivo*. However, phosphorylation of Thr$^{505}$ is not absolutely required for the PKCδ activity but may be required for its stability (27). PKCδ was also shown to be phosphorylated on several tyrosine residues in the $H_2O_2$-treated cells, which converts the enzyme into a constitutively active enzyme that is independent of DAG (25). In apoptotic cells, a catalytically active PKCδ is generated by proteolysis, which then translocates to the nucleus (9–11, 28).

The mechanisms of PKC activation by DAG and its non-physiological analogs, phorbol esters, have been extensively

* This work was supported by National Institutes of Health Grants GM52598, GM53987, and GM68849. The costs of publication of this article were defrayed in part by the payment of page charges. This article must therefore be hereby marked "*advertisement*" in accordance with 18 U.S.C. Section 1734 solely to indicate this fact.

‡ Present address: Dept. of Cell Biology, Yale University School of Medicine, P. O. Box 208002, 333 Cedar St., New Haven, CT 06520-8002.

§ To whom correspondence should be addressed: M/C 111, 845 West Taylor St., Chicago, IL 60607-7061. Tel.: 312-996-4883; Fax: 312-996-2183; E-mail: wcho@uic.edu.

[1] The abbreviations used are: PKC, protein kinase C; CHAPS, 3-[(3-cholamidopropyl)dimethylammonio]-1-propanesulfonic acid; DAG, *sn*-1,2-diacylglycerol; OPG, 1-octanoyl-2-(8-pyrenyloctanoyl)-*sn*-3-glycerol; $DiC_8$, *sn*-1,2-dioctanoylglycerol; $DiC_{18}$, *sn*-1,2-dioleoylglycerol; DMEM, Dulbecco's modified Eagle's medium; EGFP, enhanced green fluorescent protein; HEK, human embryonic kidney; ITC, isothermal titration calorimetry; POPC, 1-palmitoyl-2-oleoyl-*sn*-glycero-3-phosphocholine; POPE, 1-palmitoyl-2-oleoyl-*sn*-glycero-3-phosphoethanolamine; POPG, 1-palmitoyl-2-oleoyl-*sn*-glycero-3-phosphoglycerol; POPI, 1-palmitoyl-2-oleoyl-*sn*-glycero-3-phosphoinositol; POPS, 1-palmitoyl-2-oleoyl-*sn*-glycero-3-phosphoserine; PG, phosphatidylglycerol; PS, phosphatidylserine; SPR, surface plasmon resonance; PDBu, phorbol 12,13-dibutyrate.

studied, with a particular emphasis on elucidating the roles of three membrane targeting domains (C1A, C1B, and C2) in the membrane translocation and activation of different PKC isoforms. The C1 domain (~50 residues) is a cysteine-rich compact structure that was identified as the interaction site for DAG and phorbol ester (29–32), whereas the C2 domain (~130 residues) is an 8-stranded $\beta$ sandwich protein that is involved in $Ca^{2+}$-dependent membrane binding for conventional isoforms (33–36). As is the case with all novel PKCs, PKCδ contains the amino-terminal non-$Ca^{2+}$-binding C2 domain, followed by a pseudosubstrate region, the C1A domain, and the C1B domain in the regulatory domain and the C3 and C4 domains in the catalytic domain. It has been reported that the two C1 domains of PKCδ have disparate phorbol ester affinities and distinct roles in phorbol ester-induced PKC activation (37). Recent studies have revealed, however, that some PKC isoforms follow different mechanisms when they are activated by DAG and phorbol esters, respectively, because their C1A and C1B domains have opposite relative affinities for these ligands (38). This finding calls for the re-evaluation of the physiological relevance of previous mechanistic studies on the phorbol ester-induced activation of PKCs. To date, no systematic study on the mechanism of DAG-induced membrane binding and activation of novel PKC isoforms has been reported. On the basis of our recent mechanistic studies on conventional PKC isoforms, we undertook this study to elucidate how DAG induces the cellular membrane translocation and activation of PKCδ. *In vitro* membrane binding studies of individual membrane targeting domains (C1A, C1B, and C2) of PKCδ and the full-length PKCδ and mutants by isothermal titration calorimetry (ITC), surface plasmon resonance (SPR), and monolayer penetration analyses, as well as cellular membrane translocation measurements, reveal that PKCδ has a unique membrane binding and activation mechanism, which derives from the distinct DAG affinities of the two C1 domains and the unique conformational properties of this novel PKC isoform.

## EXPERIMENTAL PROCEDURES

*Materials*—1-Palmitoyl-2-oleoyl-*sn*-glycero-3-phosphocholine (POPC), 1-palmitoyl-2-oleoyl-*sn*-glycero-3-phosphoethanolamine (POPE), 1-palmitoyl-2-oleoyl-*sn*-glycero-3-phosphoglycerol (POPG), 1-palmitoyl-2-oleoyl-*sn*-glycero-3-phosphoinositol (POPI), 1-palmitoyl-2-oleoyl-*sn*-glycero-3-phosphoserine (POPS), cardiolipin, *sn*-1,2-dioctanoylglycerol ($DiC_8$), and *sn*-1,2-dioleoylglycerol ($DiC_{18}$) were purchased from Avanti Polar Lipids, Inc. (Alabaster, AL) and used without further purification. A fluorescent DAG analog, 1-octanoyl-2-(8-pyrenenyloctanoyl)-*sn*-glycerol (OPG), was synthesized from L-2,3-*O*-isopropyliden-*sn*-glycerol (Aldrich) as described elsewhere.[2] Phorbol 12,13-dibutyrate (PDBu), phorbol 12-myristate 13-acetate, cholesterol, fatty acid-free bovine serum albumin, Triton X-100, ATP, octyl glucoside, and CHAPS were from Sigma. Phospholipid concentrations were determined by a modified Bartlett analysis (39). [$\gamma$-$^{32}$P]ATP (3 Ci/$\mu$mol) was from Amersham Biosciences. Restriction endonucleases and enzymes for molecular biology were obtained from New England Biolabs (Beverly, MA). Pioneer L1 sensor chip was from Biacore AB (Piscataway, NJ). Dulbecco's modified Eagle's medium (DMEM) and LipofectAMINE™ were from Invitrogen. Human embryonic kidney (HEK) 293 cell line, Zeocin, and ponasterone A were from Invitrogen.

*Expression Vector Construction and Mutagenesis*—Expression vectors for the C1A and C1B domains were constructed by subcloning the C1A and C1B domain sequences of rat PKCδ into pET21d vectors (Novagen, Madison, WI) between NcoI and XhoI sites by overlap extension polymerase chain reaction (40) using Pfu polymerase (Stratagene, La Jolla, CA). These vectors are designed to introduce a carboxyl-terminal $His_6$ tag between the XhoI site and stop codon for affinity purification of expressed proteins.

Baculovirus transfer vectors encoding the cDNA of PKCδ with appropriate C1 domain mutations were generated by PCR (40) using pVL1392-PKCδ plasmid as a template. Briefly, four primers, including two complementary oligonucleotides introducing a desired mutation and two additional oligonucleotides complementary to the 5′- and 3′-ends of the PKCδ gene, respectively, were used for PCR mutagenesis. The 3′-end of the PKCδ gene was modified using a 3′-end primer that was designed to mutate the stop codon and contain a $His_6$ tag. Two DNA fragments overlapping at the mutation site were first generated and purified on an agarose gel. These two fragments were then annealed and extended to generate an entire PKCδ gene containing a desired mutation, which was further amplified by PCR. The product was subsequently purified on an agarose gel, and PKCδ was digested with NotI and EcoRI and subcloned into the pVL1392 plasmid digested with the same restriction enzymes. The mutation was verified by DNA sequencing.

The gene for the enhanced green fluorescent protein (EGFP) in the pEGFP vector (Clontech) was modified to remove the first methionine and add two amino-terminal glycine codons and an EcoRI site, and inserted into a modified pIND vector (Invitrogen) between the EcoRI site and the XhoI site to create plasmid pIND/EGFP. PKCδ and respective mutations were cloned by PCR to remove the stop codon and add two COOH-terminal glycine codons and an EcoRI site. The PCR product was digested with NotI and EcoRI and ligated into pIND/EGFP to create a carboxyl-terminal fusion with spacer sequence GGNSGG.

*Protein Expression and Purification—Escherichia coli* strain BL21(DE3) (Novagen) was used as a host for C1 domain expression. The soluble C1B domain and the insoluble C1A domain were expressed and purified as previously described (38, 41). Full-length PKCδ and mutants were expressed in baculovirus-infected Sf9 cells. The transfection of Sf9 cells with pVL1392-PKCδ constructs was performed using a BaculoGold™ transfection kit from BD Pharmingen. The plasmid DNA for transfection was prepared by using an EndoFree Plasmid Maxi kit (Qiagen) to avoid potential endotoxin contamination. Cells were incubated for 4 days at 27 °C, and the supernatant was collected and used to infect more cells for the amplification of virus. After three cycles of amplification, high-titer virus stock solution was obtained. Sf9 cells were maintained as monolayer cultures in TMN-FH medium (Invitrogen) containing 10% fetal bovine serum (Invitrogen). For protein expression, cells were grown to $2 \times 10^6$ cells/ml in 350-ml suspension cultures and infected with the multiplicity of infection of 10. The cells were then incubated for 3 days at 27 °C. For harvesting, cells were centrifuged at 1,000 × *g* for 10 min, the pellet was washed once with sodium phosphate buffer, pH 8.0, and resuspended in 25 ml of extraction buffer containing 50 mM sodium phosphate, pH 8.0, 300 mM NaCl, 10 mM imidazole, 50 $\mu$g/ml leupeptin, 1% Triton X-100, and 0.2 mM phenylmethylsulfonyl fluoride. The suspension was homogenized in a hand-held homogenizer chilled on ice. The extract was centrifuged at 50,000 × *g* for 45 min at 4 °C. One ml of nickel-nitrilotriacetic acid-agarose (Qiagen) was added to the supernatant and the mixture was incubated on ice while shaking at 80 rpm for 1 h. The mixture was poured onto a 10-ml column and the column was washed first with 20 ml of 50 mM sodium phosphate, pH 8.0, containing 300 mM NaCl and 10 mM imidazole, and subsequently with 15 ml of 50 mM sodium phosphate, pH 8.0, containing 300 mM NaCl and 15 mM imidazole. The column was washed with an additional 4 ml of the same buffer containing 20 mM imidazole. The protein was then eluted in 7 fractions of 0.5 ml of 50 mM sodium phosphate buffer containing 300 mM imidazole. Eluted fractions were then analyzed on a 10% sodium dodecyl sulfate-polyacrylamide gel. Fractions containing PKCδ were concentrated and desalted in an Ultrafree-15 centrifugal filter device (Millipore). Protein concentration was determined by the bicinchoninic acid method (Pierce).

*Determination of PKC Activity*—Activity of PKCδ was assayed by measuring the initial rate of [$^{32}$P]phosphate incorporation from [$\gamma$-$^{32}$P]ATP (50 $\mu$M, 0.6 $\mu$Ci/tube) into myelin basic protein (200 $\mu$g/ml) or protamine sulfate (200 $\mu$g/ml) (both from Sigma). The reaction mixture contained large unilamellar vesicles (0.2 mM of total lipid concentration), 0.16 M KCl, and 5 mM $MgCl_2$ in 20 mM HEPES, pH 7.4. Because PKCδ showed a high background activity toward the peptide substrate protamine sulfate in the absence of POPS, this substrate was mainly used for routine assays during purification. Reactions were started by adding 50 mM $MgCl_2$ to the mixture and incubating for 5 (protamine sulfate) or 10 min (myelin basic protein) at room temperature, they were quenched by addition of 50 $\mu$l of 5% phosphoric acid. Seventy-five $\mu$l of quenched reaction mixtures were spotted on P-81 ion-exchange paper, washed 4 times with a 5% solution of phosphoric acid, followed by one wash in 95% ethanol. Papers were transferred into scintillation vials containing 4 ml of scintillation fluid (Fisher) and radioactivity was measured by liquid scintillation counting.

*Monolayer Measurements*—Surface pressure ($\pi$) of solution in a cir-

[2] B. Ananthanarayanan and W. Cho, manuscript in preparation.

cular Teflon trough (4 cm diameter × 1 cm deep) was measured using a Wilhelmy plate attached to a computer-controlled Cahn electrobalance (model C-32) as described previously (42). Five to 10 μl of phospholipid solution in ethanol/hexane (1:9 (v/v)) was spread onto 10 ml of subphase (20 mM Tris-HCl, pH 7.4, containing 0.16 M KCl) to form a monolayer with a given initial surface pressure ($\pi_0$). The subphase was continuously stirred at 60 rpm with a magnetic stir bar. Once the surface pressure reading of the monolayer had been stabilized (after about 5 min), the protein solution (typically 70 μl) was injected into the subphase through a small hole drilled at an angle through the wall of the trough and the change in surface pressure ($\Delta\pi$) was measured as a function of time. Typically, the $\Delta\pi$ value reached a maximum after 30 min. It has been shown empirically that $\Delta\pi$ caused by a protein is mainly because of the penetration of the protein into the lipid monolayer (42). The maximal $\Delta\pi$ value at a given $\pi_0$ depended on the protein concentration and reached a saturation value. Protein concentrations in the subphase were therefore maintained above such values to ensure that the observed $\Delta\pi$ represented a maximal value. The critical surface pressure ($\pi_c$) was determined by extrapolating the $\Delta\pi$ *versus* $\pi_0$ plot to the *x* axis (43).

*Surface Plasmon Resonance Analysis*—Kinetics of vesicle-protein binding was determined by the SPR analysis using a BIAcore X biosensor system (Biacore AB). The lipid coating of the L1 chip has been described in detail previously (44–46). Before SPR measurement, the instrument was allowed to equilibrate with the buffer until the drift in signal was less than 0.3 resonance units/min. The sensor surface was then coated with lipid vesicles at a flow rate of 5 μl/min. The first flow cell was used as a control cell and was coated with 4500 resonance units of POPC. The second flow cell contained the surface coated with vesicles with varying lipid compositions (*e.g.* POPC/POPS/DiC$_{18}$ = 59:40:1) at 4500 resonance units. After lipid coating, 30 μl of 50 mM NaOH was injected at 100 μl/min three times to stabilize the lipid layer. Typically, no further decrease in SPR signal was observed after one wash cycle. After coating, the drift in signal was allowed to stabilize below 0.3 resonance units/min before any binding measurements, which were performed at 23 °C and at a flow rate of 30 μl/min. Ninety μl of protein sample was injected for an association time of 3 min, whereas the dissociation was then monitored for 10 min in running buffer. After each measurement, the lipid surface was typically regenerated with a 10-μl pulse of 50 mM NaOH. The regeneration solution was passed over the immobilized vesicle surface until the SPR signal reached the initial background value before protein injection. For data acquisition, 5 or more different concentrations (typically within a 10-fold range above or below the $K_d$) of each enzyme were used and data sets were repeated 3 or more times. When needed, the entire lipid surface was removed with a 5-min injection of 40 mM CHAPS followed by a 5-min injection of 40 mM octyl glucoside at 5 μl/min and the sensor chip was recoated for the next set of measurements. All data was analyzed using BIAevaluation 3.0 software (Biacore) to determine the rate constants of association ($k_a$) and dissociation ($k_d$) as described previously (44–46). Equilibrium dissociation constant ($K_d$) was either calculated from rate constants using an equation, $K_d = k_d/k_a$ assuming 1:1 binding, or directly determined from steady-state binding measurements as described previously (38). Mass transport was not a limiting factor in our experiments, as change in flow rate or ligand density did not affect kinetics of association and dissociation (47, 48).

*Isothermal Titration Calorimetry Measurements*—Binding of C1 domains to water-soluble PDBu or DiC$_8$ ligands were measured using a MicroCal VP isothermal titration calorimeter (MicroCal Inc., Northampton, MA) (38). Protein samples used for the titration were prepared by dialyzing overnight against 4 liters of a working buffer (20 mM Tris-HCl, pH 7.0, 50 μM $ZnSO_4$). Measurements were performed at 30 °C using the working buffer as a reference and a diluent. Protein and ligand concentrations used for each measurement varied according to the range of $K_d$ value to be determined. Binding measurements were performed with 5-μl stepwise injections of the ligand into the protein in the sample cell. Injections were continued until saturating signals were obtained. The collected data was analyzed with the Origin software (MicroCal) using a simple single-site model.

*Cell Culture*—A stable HEK293 cell line expressing the ecdysone receptor (Invitrogen) was used for all experiments (49). Cells were cultured in DMEM supplemented with 10% fetal bovine serum at 37 °C in 5% $CO_2$ and 98% humidity until 90% confluent. Cells were then passaged into 8 wells of a Lab-Tech™-chambered coverglass for later transfection and visualization. Only cells between the 5$^{th}$ and 20$^{th}$ passage were used. For transfection, 80–90% confluent cells in Lab-Tech™-chambered coverglass wells were exposed to 150 μl of unsupplemented DMEM containing 0.5 μg of endotoxin-free DNA and 1 μl of LipofectAMINE reagent for 7–8 h at 37 °C. After exposure, the transfection medium was removed, the cells were washed once with fetal bovine serum-supplemented DMEM, and overlaid with fetal bovine serum-supplemented DMEM containing Zeocin and 5 μg/ml ponasterone A to induce protein production for 16–24 h.

*Microscopy*—Microscopy data were collected on a custom-built combination laser scanning confocal and multiphoton microscope. Briefly, the 488-nm laser line from a continuous wave multiline argon ion laser (Melles Griot, Carlsbad, CA) was selected using an acoustic-optical tunable filter (NEOS, Melbourne, FL) and fiber launched into the scan head. Simultaneously, a 700-nm ultrafast, pulsed beam from a tunable Tsunami laser set up for femtosecond operation (Spectra Physics, Mountain View, CA) was spatially filtered and launched into the scan head. The two beams were combined through a custom dichroic mirror reflecting 680 nm of light, directed toward the primary dichroic mirror (Chroma Technology, Brattleboro, VT), and then toward the XY scan mirrors (model 6350, Cambridge Technologies, Cambridge, MA). The laser light was focused using a Prairie Technologies (Middleton WI) scan lens, collimated by the 1× Zeiss tube lens and directed toward a 40 × water corrected 1.2 numerical aperture Zeiss objective mounted on a Zeiss 200 M platform (Carl Zeiss Inc., Thornwood, NY). Light excited by the continuous wave 488-nm line was collected using a modified Prarie Technologies two-channel confocal detection apparatus equipped with Peltier-cooled 928P and 1477P style Hamamatsu photomutiplier tubes (Hamamatsu Corp. USA, Bridgewater, NJ). Light excited by the 700-nm ultrafast pulse was collected on a non-descanned pathway by Peltier-cooled 1477P style Hamamatsu photomutiplier tubes. All light was reflected and filtered using appropriate optics. Instrument control was accomplished using an ISS (Champaign, IL) 3-axis scanning card, ISS amplifiers, and two ISS 200 KHz analog lifetime cards. The software interface was SimFCS (Laboratory for Fluorescence Dynamics, University of Illinois, Urbana-Champaign, IL), a custom program written by Dr. Enrico Gratton and modified for control of this instrument.

All experiments were carried out at the same laser power (found to induce minimal photobleaching over 30 scans) and the same gains and offset setting on the photomultiplier tubes. Transfected cells were washed twice with HEK buffer (1 mM HEPES, pH 7.4, containing 2.5 mM $MgCl_2$, 140 mM NaCl, 5 mM KCl, and 6 mM sucrose). After washing, cells were overlaid with 150 μl of HEK buffer. Suitable cells were selected for imaging and a single image was taken for each cell before addition of OPG or DiC$_8$. Then, the translocation of protein and subcellular localization of lipid was simultaneously monitored at fixed intervals (every 20 s) after 150 μl of HEK buffer containing 0.1 mg/μl OPG (or DiC$_8$) was added. Control experiments were done with dimethyl sulfoxide. Images were analyzed using SimFCS. Specifically, regions of interest in the cytosol were defined, and the average intensity in a square (1 m × 1 μm) obtained with respect to time. Membrane intensities were determined for each frame in individual cells by extending a line from the cytosol to the outside of the cell and reading off the intensity with distance along the line. By cross-checking, markers on the diagram with a table of intensity values corresponding to the place on the line indicating the edge of the cell were averaged. Lines were drawn in at least three places in each cell, and membrane intensity was determined. These values were averaged and the resultant cytosolic intensity values were converted to a ratio for each frame: membrane/(membrane + cytosol). The values were then scaled for the entire time series from 0 to 100% of the obtained ratio for a given experiment. This allowed a comparison of ratiometric changes between experiments. Note that each experiment was repeated at least three times on a given day and was repeated at least two different days with different transfected cells.

## RESULTS

*Phosphatidylserine (PS)-specific Membrane Binding and Activation of PKCδ*—It has been long known that among different anionic phospholipids PS specifically enhances the membrane affinity and activity of PKCs (50, 51). Recently, however, it has been recognized that PS specificity can vary significantly among PKC isoforms depending on their structures and activation mechanisms. For instance, a conventional PKC, PKCγ, and a novel PKC, PKCε, have been reported to show little PS specificity (38, 52). Previous reports have indicated that PS enhances the membrane affinity and activity of PKCδ (3, 53). To see whether this effect is induced specifically by PS or nonspecifically by other anionic phospholipids, such as phos-

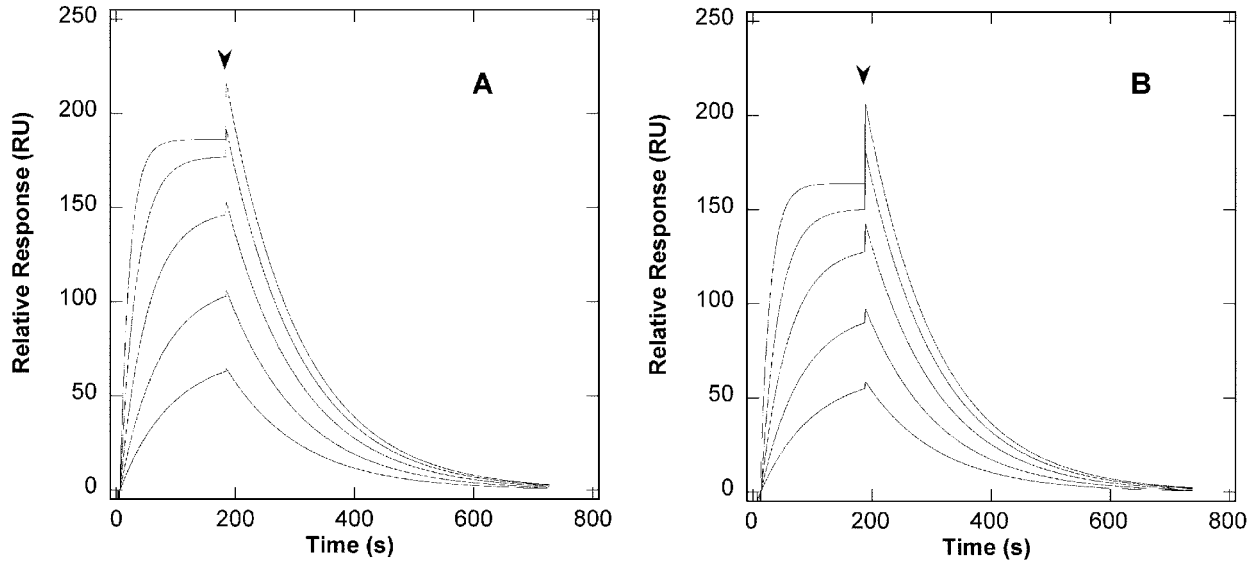


FIG. 1. **Representative sensorgrams for binding of PKCδ to vesicles.** Varying concentrations (1, 2, 4, 8, and 16 nM) of PKCδ (*A*) and EGFP-tagged PKCδ (*B*) were injected at 30 μl/min to the L1 chip coated with POPC/POPE/POPS/POPI/cholesterol/$DiC_{18}$ (12:35:22:9:21:1) vesicles and the subsequent association and dissociation were monitored. The spikes at the beginning of the dissociation phase (see the *arrows*) are because of changes in the reflective index. Data analysis showed that both proteins have essentially the same $k_a$, $k_d$, and $K_d$ values (see Table IV).

phatidylglycerol (PG), we rigorously measured the PS specificity in membrane binding and activation of PKCδ.

We first measured the binding of PKCδ to POPC/POPS/$DiC_{18}$ (59:40:1 in mole ratio) and POPC/POPG/$DiC_{18}$ (59:40:1) vesicles by the SPR analysis, which has been shown to be a powerful tool for measuring membrane-protein interactions (43, 45, 54, 55). Representative sensorgrams are shown in Fig. 1. Although 40 mol % of POPS is higher than the physiological PS concentration, this lipid composition was employed in these studies to ensure that the binding of all PKCδ proteins, including some low affinity mutants, can be quantified under the same conditions. We also employed the lowest possible concentration of $DiC_{18}$ (*i.e.* 1 mol %) that allows effective membrane binding of all PKCδ proteins to circumvent any membrane artifact caused by high DAG concentration. As listed in Table I, PKCδ exhibited a 5.5-fold higher affinity for POPC/POPS/$DiC_{18}$ (59:40:1) vesicles than for POPC/POPG/$DiC_{18}$ (59:40:1) vesicles, showing that PKCδ is selective for PS at least over PG in membrane binding. The higher affinity for PS-containing vesicles is attributed to a 1.7-fold increase in $k_a$ and a 3.2-fold decrease in $k_d$. It has been shown that membrane dissociation is slowed by short-range specific interactions or hydrophobic interactions achieved by the membrane penetration of protein (45, 56, 57). Thus it appears that the serine head group of PS interacts specifically with PKCδ or is able to facilitate membrane penetration of protein (or both). In this regard, PKCδ is more similar to a conventional PKC, PKCα, than to a novel PKC, PKCε (44, 52), despite the fact that PKCδ is a novel PKC with a non-$Ca^{2+}$-binding C2 domain.

To further investigate the effect of PS on the membrane penetration of PKCδ, we measured the interactions of PKCδ with various lipid monolayers (43). In this study, we monitored $\Delta\pi$ caused by the penetration of PKCδ to POPC/POPS and POPC/POPG mixed monolayers with varying surface packing density (*i.e.* different $p_0$). The resulting $\Delta\pi$ *versus* $\pi_0$ plots (Fig. 2) show that PKCδ is able to penetrate PS-containing monolayers more effectively than PG-containing monolayers. This indicates that PS can specifically induce the membrane penetration of PKCδ, as was the case with PKCα (52). When compared with PKCα, however, PKCδ required a higher POPS concentration to exhibit comparable monolayer penetration; *i.e.* >40 mol % of POPS was needed for PKCδ to penetrate the monolayer with $\pi_0 > 30$ dyne/cm and to fully express PS selectivity, whereas PKCα was able to penetrate the POPC/POPS (70:30) monolayer with $\pi_0 > 30$ dyne/cm (52). Thus, PKCδ is similar to PKCα in that PS can specifically induce its membrane penetration but is different from PKCα in that a significantly higher concentration of PS is required for PKCδ to penetrate the densely packed membrane. It was reported that DAG does not affect the monolayer penetration *per se* of PKCα, although greatly enhancing its membrane affinity (52, 58). Similarly, $DiC_{18}$ did not directly affect the penetration of PKCδ into the POPC/POPS (50:50) monolayer (data not shown).

We also measured the kinase activity of PKCδ in the presence of PS- and PG-containing vesicles, *i.e.* POPC/POPS(G)/$DiC_{18}$ ((99-*x*):*x*:1). Fig. 3 clearly shows that PKCδ is activated much more readily by PS-containing vesicles than PG-containing vesicles; the maximal activity achieved with PG-containing vesicles reaches only 20% of that achieved with PS-containing vesicles. Again, this behavior is similar to that of PKCα, but is in sharp contrast to that of PKCε, which is activated equally well by PS- and PG-containing vesicles (52). Collectively, these results indicate that membrane binding affinity and activity of PKCδ are selectively enhanced by PS.

*Role of C2 Domain in Membrane Binding and Activation of PKCδ*—It has been well established that the C2 domains of conventional PKCs are involved in the $Ca^{2+}$-dependent membrane binding and activation of these PKCs (33, 59, 60). However, the role of non-$Ca^{2+}$-binding C2 domains of novel PKCs remains unclear. Recent studies have indicated that the C2 domain of PKCε may be involved in membrane binding. For instance, Ochoa *et al.* (61) reported that the C2 domain of PKCε could interact nonspecifically with anionic phospholipids, whereas Pepio *et al.* (62) reported that phosphorylation of $Ser^{36}$ in the C2 domain of PKC *Aplysia* II, which is more closely related to mammalian PKCε than to PKCδ, promoted the membrane interaction of the C2 domain. The C2 domain of PKCδ shares only 16% homology with that of PKCε and major differences are found in their tertiary structures, particularly in the loop regions (61, 63, 64). To see if the C2 domain plays any role in the membrane binding of PKCδ, we measured the membrane binding properties of isolated C2 domain of PKCδ and also

TABLE I
*Membrane binding parameters for PKCδ and mutants determined from SPR analysis*
Values represent the mean ± S.D. from five determinations. All measurements were performed in 10 mM HEPES, pH 7.4, containing 0.16 M KCl.

| Proteins | $k_a$ | $k_d$ | $K_d$ | PS selectivity[a] |
|---|---|---|---|---|
| | $M^{-1}\ s^{-1}$ | $s^{-1}$ | $M$ | |
| POPC/POPS/DiC$_{18}$ (59:40:1) | | | | |
| PKCδ | $(1.4 \pm 0.3) \times 10^5$ | $(9.3 \pm 0.8) \times 10^{-4}$ | $(6.6 \pm 1.0) \times 10^{-9}$ | |
| E177A | $(4.7 \pm 0.6) \times 10^5$ | $(2.5 \pm 0.4) \times 10^{-4}$ | $(5.3 \pm 1.1) \times 10^{-10}$ | |
| W180G | $(4.0 \pm 0.7) \times 10^4$ | $(2.0 \pm 0.4) \times 10^{-3}$ | $(5.0 \pm 1.3) \times 10^{-8}$ | |
| L182G | $(1.7 \pm 0.4) \times 10^5$ | $(6.2 \pm 1.0) \times 10^{-3}$ | $(3.6 \pm 1.0) \times 10^{-8}$ | |
| D245A | $(2.4 \pm 0.8) \times 10^5$ | $(6.0 \pm 0.6) \times 10^{-4}$ | $(2.5 \pm 0.9) \times 10^{-9}$ | |
| W252G | $(1.8 \pm 0.5) \times 10^5$ | $(1.3 \pm 0.1) \times 10^{-3}$ | $(7.2 \pm 2.0) \times 10^{-9}$ | |
| L254G | $(1.3 \pm 0.2) \times 10^5$ | $(9.9 \pm 0.7) \times 10^{-4}$ | $(7.6 \pm 1.0) \times 10^{-9}$ | |
| C2 deletion | $(1.6 \pm 0.5) \times 10^5$ | $(6.2 \pm 0.8) \times 10^{-4}$ | $(4.6 \pm 2.0) \times 10^{-9}$ | |
| POPC/POPG/DiC$_{18}$ (59:40:1) | | | | |
| PKC-δ | $(8.3 \pm 0.5) \times 10^4$ | $(3.0 \pm 0.5) \times 10^{-3}$ | $(3.6 \pm 0.7) \times 10^{-8}$ | 5.5 |
| E177A | $(4.5 \pm 0.6) \times 10^5$ | $(5.0 \pm 0.6) \times 10^{-4}$ | $(1.1 \pm 2.0) \times 10^{-9}$ | 2.1 |
| D245A | $(3.2 \pm 0.5) \times 10^5$ | $(6.4 \pm 0.6) \times 10^{-4}$ | $(2.0 \pm 0.4) \times 10^{-9}$ | 0.8 |
| C2 deletion | $(8.8 \pm 0.9) \times 10^4$ | $(2.5 \pm 0.3) \times 10^{-3}$ | $(2.8 \pm 0.4) \times 10^{-8}$ | 6.1 |

[a] PS selectivity is defined as the ratio of $(1/K_d)$ for POPC/POPS/DiC$_{18}$ (59:40:1) to $(1/K_d)$ for POPC/POPG/DiC$_{18}$ (59:40:1).

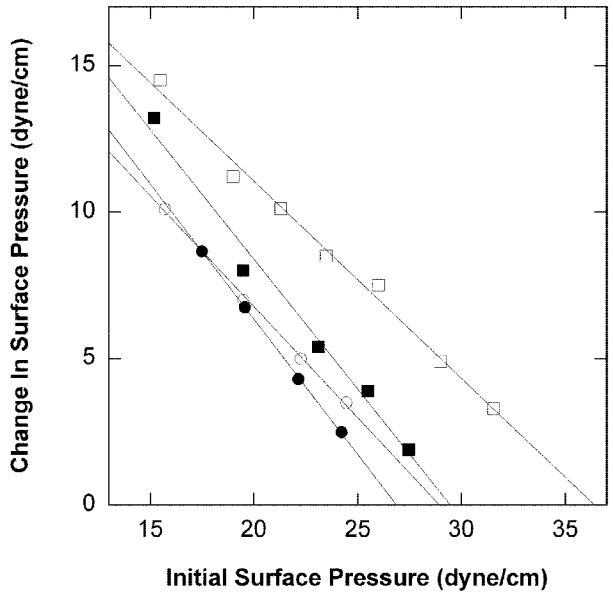


FIG. 2. **Monolayer penetration of PKCδ.** $\Delta\pi$ was measured as a function of $\pi_0$ for PKCδ wild type with POPC/POPS (7:3) (○), POPC/POPG (7:3) (●), POPC/POPS (5:5) (□), and POPC/POPG (5:5) (■) monolayers. The subphase was 20 mM Tris buffer, pH 7.4, containing 0.16 M KCl.

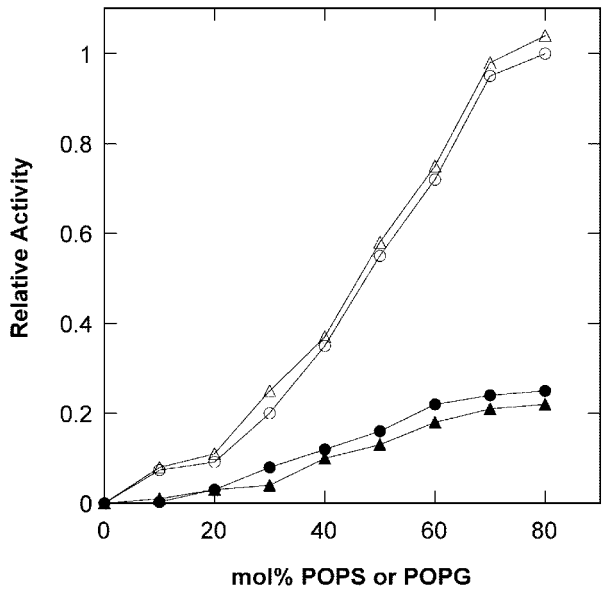


FIG. 3. **Enzymatic activity of PKCδ and the C2 deletion mutant in the presence of POPC/POPS(G)/DiC$_{18}$ vesicles.** The kinase activity of 30 nM PKCδ (*circles*) and its C2 deletion mutant (*triangles*) was measured in the presence of 0.2 mM POPC/POPS/DiC$_{18}$ (99-*x*:*x*:1) (*open symbols*) or POPC/POPG/DiC$_{18}$ (99-*x*:*x*:1) (*filled symbols*) vesicles in 20 mM HEPES buffer, pH 7.4, containing 0.16 M KCl, 5 mM $MgCl_2$, and myelin basic protein (200 μg/ml). Each data point represents an average of duplicate measurements. Relative activity was calculated in comparison with the maximal activity of wild type achieved with PS vesicles.

measured the effect of the C2 domain deletion on membrane binding and activation of full-length PKCδ. The isolated C2 domain of PKCδ (with up to 50 μM protein) exhibited no detectable binding to POPC/POPS, POPC/POPG, or POPC/POPA mixed vesicles containing up to 50% anionic phospholipids in the SPR analysis. Furthermore, the C2 deletion had only small effects on the vesicle binding (Table I) or activation (Fig. 3) of the full-length protein, indicating that this C2 domain does not play a direct role in the DAG-dependent membrane binding and activation of PKCδ.

*Differential DAG Affinity of C1A and C1B Domains*—Our previous studies indicated that the C1A domain plays a critical role in the DAG-induced membrane binding and activation of PKCα (38, 65), whereas both the C1A and C1B domains of PKCγ participate in these processes (38). This is ascribed to the fact that the C1A domain of PKCα has higher DAG affinity, whereas both the C1A and C1B domains of PKCγ have comparable DAG affinity and conformational flexibility. Roles of the C1A and C1B domains in the phorbol ester-induced activation of novel PKCs have been extensively studied (37, 66–71). The affinity of isolated C1A and C1B domains of novel PKCs for phorbol esters has also been measured (72, 73). However, no systematic study has been reported on the physiologically more relevant DAG-induced activation of novel PKCs. Because it was shown that the principles learned from the phorbol ester-mediated activation of a PKC isoform may not be applied to the DAG-mediated activation of the PKC (38), it is necessary to measure the relative DAG affinity of the C1A and C1B domains and their relative contribution to DAG-induced novel PKC activation to fully understand the mechanism of DAG-induced activation of novel PKC.

To achieve this goal, we first expressed the isolated C1 and C2 domains of PKCδ. The C1B domain was expressed as soluble protein in *E. coli*, whereas the C1A domain was expressed as inclusion bodies, which were then solubilized in urea and refolded. To verify that the C1A and C1B domains of PKCδ

TABLE II
*Phorbol ester binding parameters for PKCδ C1 domains determined from ITC and SPR analyses*

Values represent the mean ± S.D. from three determinations. All measurements were performed in 10 mM HEPES, pH 7.4, containing 0.16 M KCl unless specified otherwise.

| Proteins | PDBu, literature[a], $K_d$ | PDBu, ITC analysis | | PMA[b], SPR analysis, $K_d$ |
|---|---|---|---|---|
| | | Stoichiometry | $K_d$ | |
| | *nM* | *nM* | | *nM* |
| PKCδ-C1A | ~300 | NM[c] | NM | 360 ± 21 |
| PKCδ-C1B | 1.0 ± 0.1 | 0.96 ± 0.01 | 58 ± 26 | 40 ± 4 |

[a] Taken from Ref. 73.
[b] POPC/POPS/phorbol 12-myristate 13-acetate (69.95:30:0.05) vesicles.
[c] NM, not measurable.

TABLE III
*DAG binding parameters for PKCδ C1 domains determined from ITC and SPR analyses*

Values represent the mean ± S.D. from three determinations. All measurements were performed in 10 mM HEPES, pH 7.4, containing 0.16 M KCl unless specified otherwise.

| Proteins | $DiC_8$ (ITC analysis) | | $DiC_{18}$[a](SPR analysis), $K_d$ |
|---|---|---|---|
| | Stoichiometry | $K_d$ | |
| | | *nM* | *nM* |
| PKCδ-C1A | 0.91 ± 0.05 | 85 ± 27 | 30 ± 2 |
| PKCδ-C1B | NM[b] | NM | 7800 ± 1800 |

[a] POPC/POPS/$DiC_{18}$ (67.5:30:2.5) vesicles.
[b] NM, not measurable.

were correctly folded, their affinity for PDBu was measured by ITC. The values of $K_d$ and stoichiometry for C1-PDBu binding are summarized in Table II. The C1A domain had no detectable affinity for PDBu, whereas the C1B domain bound PDBu with a $K_d$ of 58 nM. This value is higher than the reported $K_d$ for the C1B domain because the latter value was determined in the presence of PS vesicles (73).

We then determined by ITC analysis the affinity of the C1A and C1B domains for a short-chain DAG analog, $DiC_8$, which was shown to exist as a monomer in the concentration range (10–100 nM) used for this binding study (38). As shown in Table III, the C1A domain bound $DiC_8$ with a $K_d$ of 85 nM, whereas the C1B domain showed no detectable binding. Thus, as was the case with PKCα (38, 74), the C1A and C1B domains of PKCδ have opposite affinities for DAG and phorbol ester, *i.e.* the C1A domain with high affinity for DAG and the C1B domain with high affinity for phorbol ester. We also measured the binding of C1A and C1B domains to DAG and phorbol ester with longer acyl chains that are incorporated in the lipid bilayer. First, the affinity of C1 domains was measured for POPC/POPS/$DiC_{18}$ (67.5:30:2.5) vesicles by SPR analysis. The C1B domain exhibited lower affinity for the $DiC_{18}$-containing vesicles than the C1A domain by 260-fold, showing that the C1A domain has much higher affinity for DAG, whether it is in solution or in the membrane. Similarly, the C1B domain bound to POPC/POPS/phorbol 12-myristate 13-acetate (69.95:30:0.05) vesicles with 9-fold higher affinity than the C1A domain, underscoring the high affinity of the C1B domain for both soluble and membrane-incorporated phorbol esters. Collectively, these data suggest that because of its much higher affinity for DAG the C1A domain should play a predominant role in the DAG-mediated membrane binding and activation of PKCδ.

*Differential Roles of C1A and C1B Domains in PKCδ Activation*—To test the notion that the C1A domain plays a major role in the DAG-mediated membrane binding and activation of PKCδ, we measured the effects of selected mutations of the C1A and C1B domains of PKCδ on its membrane binding and activation. Mutations were made on hydrophobic residues whose counterparts in conventional PKCs have been shown to be important for their membrane binding (38, 65); *i.e.* W180G and L182G for the C1A domain and W252G and L254G for the C1B domain. First, the activity measurements of these mutants in the presence of POPC/POPS/$DiC_{18}$ ((99-*x*):*x*:1) vesicles showed that the C1A domain mutants, W180G and L182G, had much lower activity than wild type and C1B domain mutants, W252G and L254G (Fig. 4). In accordance with this, W180G and L182G had 8- and 6-fold lower affinity for POPC/POPS/$DiC_{18}$ (59:40:1) vesicles than wild type, respectively, whereas W252G and L254G had wild type-like vesicle affinity (see Table I). Both W180G and L182G exhibited an increase in $k_d$, which is consistent with the putative involvement of the mutated

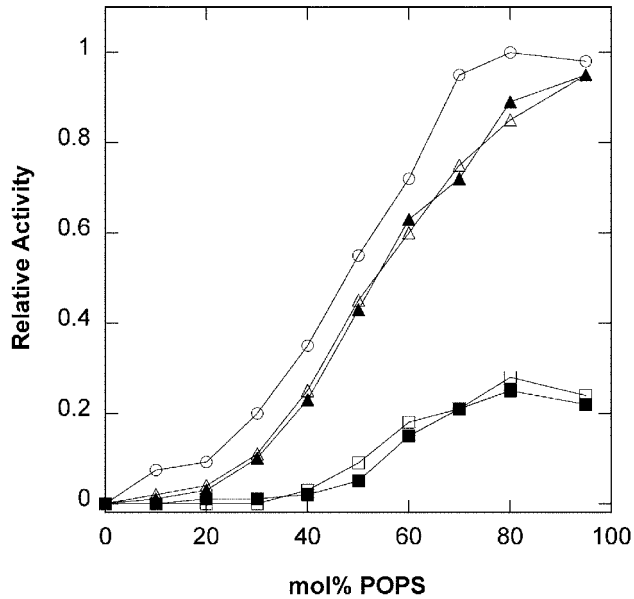


FIG. 4. **Enzymatic activity of PKCδ and C1 domain hydrophobic site mutants in the presence of POPC/POPS/$DiC_{18}$ vesicles.** Wild type (○), W180G (□), L182G (■), W252G (△), and L254G (▲) were employed with POPC/POPS/$DiC_{18}$ (99-*x*:*x*:1) vesicles. Experimental conditions were the same as described in the legend to Fig. 2.

hydrophobic residues in membrane penetration (45, 56, 57). Monolayer measurements further supported this notion. The C1A domain mutations greatly reduced monolayer penetration, whereas the C1B domain mutation (W252G) had a smaller effect (see Fig. 5). Interestingly, the C1A domain mutants had much reduced activity even under the condition where they were expected to be fully vesicle-bound (*i.e.* with 0.2 mM of POPC/POPS/$DiC_{18}$ vesicles containing >40 mol % PS; see Fig. 4), suggesting that the membrane penetration and correct positioning of the C1A domain is important not only for membrane binding but also for optimal PKCδ activation.

*Origin of PS Specificity*—We previously showed that $Asp^{55}$ in the C1A domain of PKCα is involved in tethering of the C1A domain to the other part of the PKC molecule (44). It was postulated that the PS specificity of PKCα activation derives from the release of the tethering by PS that binds to the C2 domain (and possibly other parts) of PKCα (44). PKCδ has $Glu^{177}$ in place of $Asp^{55}$ of PKCα but its C2 domain shows no affinity for PS (see Table I), suggesting that PKCδ might achieve PS specificity by a different mechanism. To test this notion, we replaced $Glu^{177}$ in the C1A domain and its counterpart in the C1B domain, $Asp^{245}$, by Ala and measured vesicle binding, monolayer penetration, and kinase activity of mutants.

SPR vesicle binding measurements showed that E177A and D245A bound to POPC/POPS/$DiC_{18}$ (59:40:1) vesicles 12- and 2.6-fold, respectively, more strongly than wild type (see Table

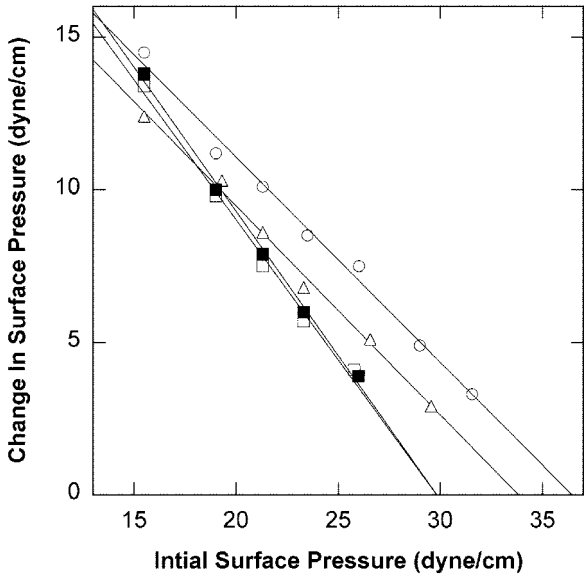


FIG. 5. **Monolayer penetration of PKCδ and C1 domain hydrophobic site mutants.** $\Delta\pi$ was measured as a function of $\pi_0$ for PKCδ wild type (○), W180G (□), L182G (■), and W252G (△) with the POPC/POPS (5:5) monolayer. The subphase was 20 mM Tris buffer, pH 7.4, containing 0.16 M KCl.

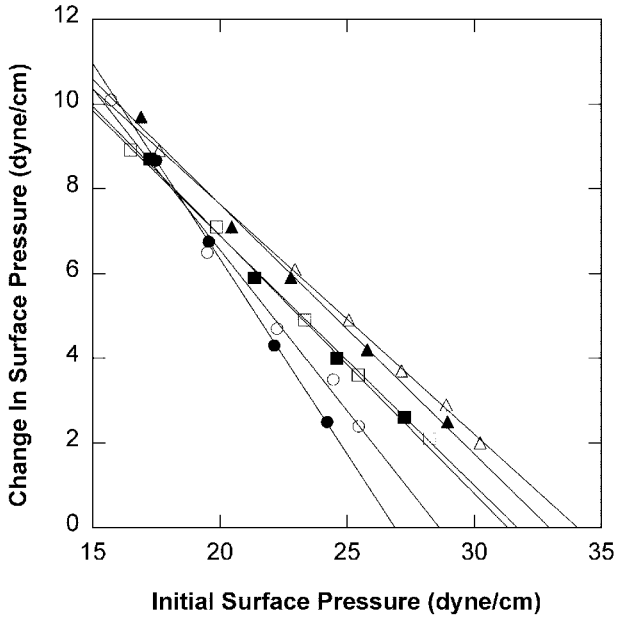


FIG. 6. **Monolayer penetration of PKCδ and C1 domain anionic site mutants.** Wild type (*circles*), E177A (*triangles*), and D245A (*squares*) were used with POPC/POPS (7:3) (*open symbols*) and POPC/POPG (7:3) monolayers (*filled symbols*). The subphase was 20 mM Tris buffer, pH 7.4, containing 0.16 M KCl.

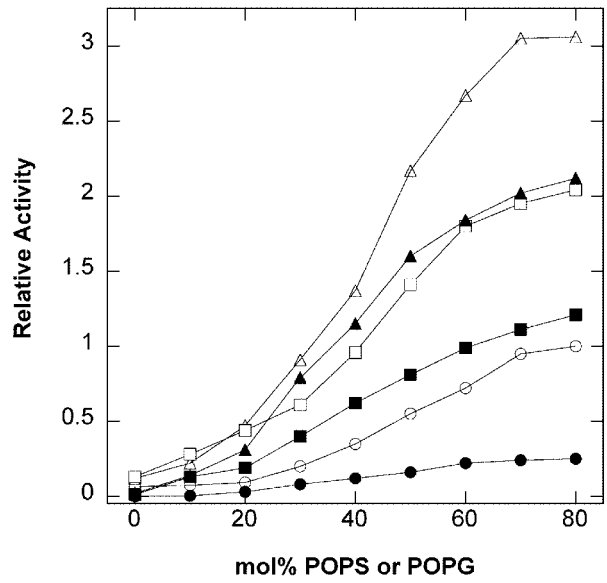


FIG. 7. **Enzymatic activity of PKCδ and C1 domain anionic site mutants in the presence of POPC/POPS(G)/DiC$_{18}$ vesicles.** Wild type (*circles*), E177A (*triangles*), and D245A (*squares*) were used with POPC/POPS/DiC$_{18}$ (99-*x*:*x*:1) (*open symbols*) and POPC/POPG/DiC$_{18}$ (99-*x*:*x*:1) (*filled symbols*) vesicles. Experimental conditions were the same as in Fig. 2.

I). Importantly, both E177A and D245A showed even more greatly enhanced affinity for POPC/POPG/DiC$_{18}$ (59:40:1) vesicles. As a result, both mutants exhibited much reduced PS selectivity; *i.e.* E177A showed only 2.1-fold preference for PS-containing vesicles, and D245A actually had slightly higher affinity for PG-containing vesicles. Interestingly, both mutations not only increase $k_a$ but also decrease $k_d$ in vesicle binding to both PS- and PG- containing vesicles. Thus, the mutations did not simply enhance nonspecific electrostatic binding to anionic vesicles by removing an anionic residue. It is more likely that the mutations facilitate membrane penetration of PKCδ by unleashing its C1 domains. To test this notion, we measured the penetration of E177A and D245A into POPC/POPS (7:3) and POPC/POPG (7:3) monolayers. As shown in Fig. 6, both E177A and D245A were able to penetrate the POPC/POPS (7:3) and POPC/POPG (7:3) monolayers more effectively than wild type.

We also measured the activity of wild type and mutants as a function of anionic lipid composition in POPC/POPS(G)/DiC$_{18}$ (99-*x*:*x*:1) vesicles. As shown in Fig. 7, both E177A and D245A showed higher activity than wild type at any given POPS (or POPG) concentration. Also, E177A and D245A, E177A in particular, only modestly (*i.e.* <2-fold) favored POPS over POPG, whereas the wild type showed high PS selectivity in the whole range of anionic phospholipid concentration used in these measurements. Thus, it appears that both Glu$^{177}$ in the C1A domain and Asp$^{245}$ in the C1B domain are involved in PS specificity in both membrane binding and activation of PKCδ.

*Cellular Membrane Translocation*—To understand how *in vitro* DAG-dependent membrane binding properties of PKCδ affects its cellular membrane targeting, we monitored the DAG-dependent subcellular translocation of PKCδ and selected mutants, each tagged with EGFP, in HEK293 cells. Control SPR experiments showed that PKCδ with the EGFP tag at the carboxyl terminus had the affinity for POPC/POPS/DiC$_{18}$ (59:40:1) vesicles that was comparable with their non-EGFP-tagged counterparts employed in *in vitro* studies (see Fig. 1). Furthermore, the cellular level of expression of different protein constructs was comparable in most cells when assessed by Western blotting using PKCδ-specific antibodies (data not shown). Finally, a visual inspection did not show obvious signs of apoptosis, such as rounding of cells and bleb formation, in any HEK293 cells expressing PKCδ and mutants under our experimental conditions.

Membrane translocation of EGFP-tagged PKCδ and mutants was induced by treating transfected HEK293 cells with 0.1 mg/ml short-chain DAGs, OPG, or DiC$_8$, because they are much more readily distributed to intracellular membranes than DiC$_{18}$. In particular, fluorogenic OPG allowed us to monitor the time lapse location of DAG and PKCδ simultaneously. This is important because the cellular spatiotemporal dynamics of

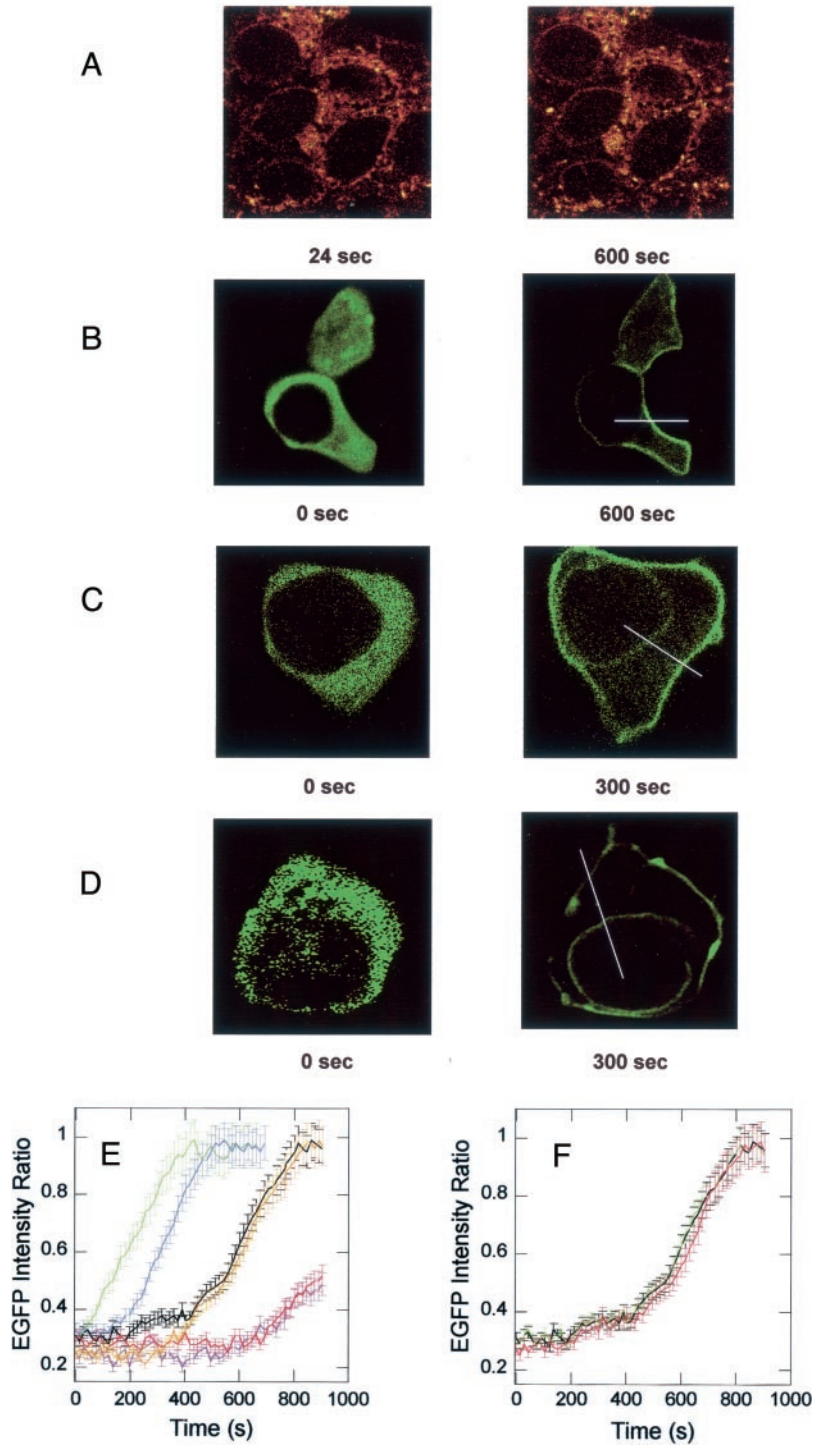


FIG. 8. **Membrane translocation and cellular distribution of EGFP-tagged PKCδ and mutants in response to OPG treatment.** *A–D*, cells were treated with 0.1 mg/ml OPG and two-photon images of OPG (*A*), PKCδ wild type (*B*), E177A (*C*), and D245A (*D*) were taken every 20 s. Each image is a representative from 20 to 25 cells, most of which behaved similarly. *Lines* shown here represent one of three lines drawn in each cell for calculating subcellular distribution of EGFP intensity (see Fig. 9). *E*, the time-lapse changes in EGFP intensity ratio at the plasma membrane (= plasma membrane/(plasma membrane + cytoplasm)) are shown for PKCδ wild type (*black*), E177A (*green*), W180G (*purple*), L182G (*red*), D245A (*blue*), W252G (*yellow*), and L254G (*orange*). *F*, effects of 0.5 μM colcemide (*red*) and 1 μM cytochalasin D (*green*) on PKCδ translocation rates. Translocation of PKCδ without inhibitors is shown in *black*. *Error bars* are from independent measurements of different cells.

PKCδ would follow that of DAG. For monitoring OPG, two-photon excitation was essential for exciting and circumventing the photobleaching of the pyrene probe. Fig. 8 shows the time lapse images of OPG and EGFP-tagged proteins in representative cells. A minimum of quadruple measurements were performed for each protein with >5 cells monitored for each measurement. Typically, >80% of the cell population showed similar behaviors with respect to DAG-induced PKCδ translocation. Because its lipophilicity is lower than that of natural DAGs with longer acyl chains, OPG was rapidly distributed to all cellular membranes within 30 s when added to the cells (Fig. 8*A*). Interestingly, wild type PKCδ translocated exclusively to the plasma membrane even when OPG was found in other intracellular membranes (Fig. 8*B*). Quantitative evaluation of the cellular distribution of EGFP intensity throughout the cell (see Fig. 9*A*) demonstrates the predominant EGFP population at the plasma membrane. These results suggest that the PS specificity of PKCδ might govern its specific targeting to the PS-rich plasma membrane. This notion is further supported by the dual subcellular localization pattern of E177A and D245A, which have much more reduced PS specificity than wild type. Cell images (Fig. 8, *B* and *C*) and fluorescence intensity profiles (Fig. 9, *B* and *C*) indicate that significant portions of these mutants are localized to the nuclear membrane. Similar results were obtained when HEK293 cells were activated by $DiC_8$ in lieu of OPG (data not shown).

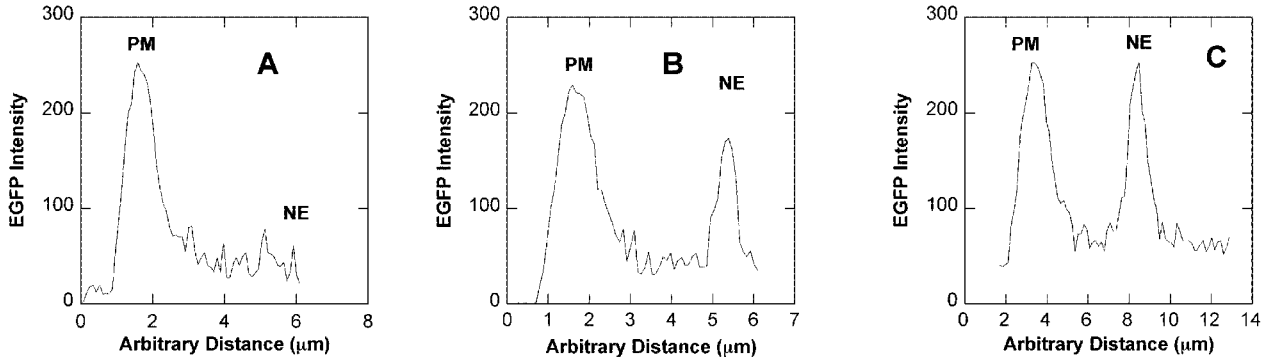


FIG. 9. **Subcellular distribution of EGFP intensity after OPG addition to HEK293 cells.** EGFP intensity profiles were determined from Fig. 8 as described under "Experimental Procedures." The differential subcellular localization patterns are shown for PKCδ wild type (*A*), E177A (*B*), and D245A (*C*) 10 min after OPG addition. *PM* and *NE* indicate plasma membrane and nuclear envelope, respectively.

We previously showed that many cellular proteins exhibiting specific targeting to the plasma membrane have pronounced specificity for the vesicles whose lipid head group composition recapitulates that of the cytoplasmic leaflet of plasma membrane over vesicles with the lipid compositions of other intracellular membranes, such as nuclear membrane (49). To see if differential subcellular targeting behaviors of PKCδ and the two mutants truly reflect their lipid head group specificity, we measured their binding to vesicle mimics of the plasma membrane and nuclear membrane (49) containing 1 mol % $DiC_{18}$ by the SPR analysis. These mimics are designed to recapitulate the lipid head group compositions, but not the acyl group compositions, of cell membranes. As listed in Table IV, PKCδ binds the plasma membrane mimic 50-fold more strongly than the nuclear membrane mimic. Interestingly, E177A and D245A exhibited significantly reduced specificity for the plasma membrane mimic when compared with the wild type. In agreement with the loss of PS specificity data, E177A binds only 6-fold more strongly to the plasma membrane mimic than the nuclear membrane mimic, whereas D245A exhibits a similar loss of specificity for the plasma membrane with 6-fold higher affinity for the plasma membrane mimic compared with the nuclear membrane mimic. These binding measurements support the notion that the differential subcellular distribution of PKCδ and mutants derives at least in part from their different lipid head group specificity.

We also determined the rates of OPG (or $DiC_8$)-induced plasma membrane translocation for wild type and mutants to evaluate the correlation between their *in vitro* vesicle affinity and cellular membrane translocation efficiency. Good correlation has been observed between the *in vitro* vesicle affinity of membrane targeting domains and their cellular membrane translocation rates (49). The analysis of EGFP intensity *versus* time plots showed that E177A and D245A had significantly faster rates of translocation to the plasma membrane than wild type (see Fig. 8*E*), respectively, which is in accordance with their higher affinity for the plasma membrane mimic than wild type. This also supports the notion that both E177A and D245A are less conformationally restricted than wild type and thus can bind DAG-containing membranes more readily. Fig. 8*E* seems to indicate that E177A and D245A have essentially the same degrees of plasma membrane translocation as wild type despite their higher membrane affinity. It should be noted, however, that they show dual targeting to plasma and nuclear membranes and that the total extent of membrane translocation for these mutants are significantly higher than that of wild type. We also found that the C1B hydrophobic site mutants (W252G and L254G) behaved like wild type, whereas C1A domain mutants (W180G and W182G) translocated significantly more slowly and less extensively to the plasma membrane than wild type (see Fig. 8*E*), which is again consistent with our *in vitro* membrane binding data. Thus, it would seem that the C1A domain plays the same major role in both *in vitro* and cellular DAG-mediated membrane translocation of PKCδ.

Last, we measured the effects on PKCδ translocation of an actin polymerization inhibitor (cytochalasin D) and a microtubule depolymerizing compound (colcemide) to see if the interaction of PKCδ with cytoskeletal proteins is important for its specific plasma membrane targeting as proposed previously (75). Under our experimental conditions, pretreatment of HEK293 cells for 1 h with neither cytochalasin D (up to 1 μM) nor colcemide (up to 0.5 μM) had any detectable effect on the subcellular localization of PKCδ and mutants (see Fig. 8*F*).

## DISCUSSION

The present study illustrates how three membrane targeting domains (C1A, C1B, and C2 domains) of PKCδ mediate its membrane binding and activation in response to DAG. Our characterization of the isolated C2 domain of PKCδ and the C2 deletion mutant indicate that the C2 domain is not directly involved in either membrane binding or enzyme activation. It is still possible, however, that the C2 domain serves as a protein-protein interaction site in the cell, as previously proposed (75, 76). The isolated C1A domain of PKCδ has much higher DAG affinity than the C1B domain, and thus under physiologically relevant conditions only the C1A domain is expected to bind DAG. In accordance with this notion, mutations of hydrophobic residues in the C1A domain greatly reduced the affinity of PKCδ for DAG-containing vesicles and its enzyme activity in the presence of DAG-containing vesicles, whereas corresponding mutations in the C1B had much smaller effects. In particular, a C1A domain mutant, W180G, has only 20% of wild type activity even with high PS concentrations in vesicles. Our monolayer penetration data, in conjunction with the SPR vesicle binding data showing that the C1A domain hydrophobic site mutations reduce the vesicle affinity of PKCδ mainly by $k_d$, indicate that membrane penetration of the C1A domain is an essential step in its function in membrane binding and activation of PKCδ. Our measurements also showed that the C1B domain of PKCδ has higher affinity for phorbol esters than the C1A domain, which is consistent with previous reports showing the importance of the C1B domain in phorbol ester-induced membrane targeting and activation of PKCδ (67). Therefore, these data represent another example demonstrating disparate mechanisms for DAG- and phorbol ester-induced PKC activation (38).

As is the case with PKCα, PKCδ exhibits definite PS selectivity in vesicle binding and kinase activity. Our previous study on PKCα (44) indicated that $Asp^{55}$ of the C1A domain of PKCα

TABLE IV
*Affinity of PKCδ and mutants for cell membrane mimics determined from SPR analysis*
Values represent the mean ± S.D. from three determinations. All measurements were performed in 10 mM HEPES, pH 7.4, containing 0.16 M KCl.

| Proteins | $k_a$ | $k_d$ | $K_d$ | PM specificity[a] |
|---|---|---|---|---|
| | $M^{-1}\ s^{-1}$ | $s^{-1}$ | $M$ | |
| Plasma membrane mimic: POPC/POPE/POPS/ POPI/cholesterol/$DiC_{18}$ (12:35:22:9:21:1) | | | | |
| PKCδ | $(3.4 \pm 0.5) \times 10^6$ | $(8.0 \pm 0.7) \times 10^{-3}$ | $(2.4 \pm 0.4) \times 10^{-9}$ | |
| E177A | $(1.1 \pm 0.3) \times 10^7$ | $(1.2 \pm 0.3) \times 10^{-3}$ | $(1.1 \pm 0.4) \times 10^{-10}$ | |
| D245A | $(5.5 \pm 0.5) \times 10^6$ | $(1.5 \pm 0.2) \times 10^{-3}$ | $(2.7 \pm 0.4) \times 10^{-10}$ | |
| Nuclear membrane mimic: POPC/POPE/POPS/ POPI/cholesterol/$DiC_{18}$ (61:21:4:7:6:1) | | | | |
| PKCδ | $(3.8 \pm 0.6) \times 10^5$ | $(4.5 \pm 0.3) \times 10^{-2}$ | $(1.2 \pm 0.2) \times 10^{-7}$ | 50 |
| E177A | $(5.9 \pm 0.5) \times 10^6$ | $(4.3 \pm 0.6) \times 10^{-3}$ | $(7.0 \pm 1.1) \times 10^{-10}$ | 6 |
| D245A | $(3.8 \pm 0.4) \times 10^6$ | $(5.5 \pm 0.7) \times 10^{-3}$ | $(1.5 \pm 0.2) \times 10^{-9}$ | 6 |

[a] Ratio of $(1/K_d)$ for the plasma membrane mimic to $(1/K_d)$ for the nuclear membrane mimic.

is involved in tethering of the C1A domain to the PKC molecule and that this tethering is released specifically by PS, hence the PS specificity. The mutation of $Asp^{55}$ of PKCα to Ala, which releases the tether, significantly enhances the *in vitro* and cellular membrane affinity and activity of PKCα and dramatically lowers its PS selectivity. For PKCγ with no PS selectivity and specificity, however, the mutation of its C1A domain anionic residue that corresponds to $Asp^{55}$ of PKCα had no effect on the DAG-induced membrane binding and activation of PKCγ (38). The present study shows that the mutation of $Glu^{177}$, which corresponds to $Asp^{55}$ of PKCα, to Ala dramatically improves membrane affinity, activation, and monolayer penetration capability of PKCδ and greatly reduces PS selectivity. Therefore, it would seem that PS specifically disrupts the $Glu^{177}$-mediated C1A domain tethering and thereby induces membrane penetration and activation of PKCδ.

For PKCα, the mutation of $Asp^{116}$ in the C1B domain had minor effects on its vesicle and enzyme activity under specific conditions, *i.e.* in the presence of PS- and DAG-containing vesicles, but significantly enhanced the enzyme activity under nonspecific conditions, *e.g.* in the presence of PG-containing vesicles or at lower calcium concentrations (44). This suggested that the residue might play a role in restricting the mobility of the C1B domain and thereby suppressing nonspecific activation, although it is not directly involved in enzyme activation or PS specificity (44). In contrast, the mutation of $Asp^{116}$ of PKCγ had no detectable effect, because of the conformationally free nature of the C1 domains in PKCγ (38). Our mutational analysis indicates that $Asp^{245}$ of the C1B domain of PKCδ might be more directly involved in enzyme activation and PS specificity than $Asp^{116}$ of PKCα. D245A of PKCδ has 2.6-fold higher affinity for POPC/POPS/$DiC_{18}$ (59:40:1) vesicles than wild type (Table I), has about 2-fold higher activity than wild type in the presence of PS-containing vesicles (Fig. 7), penetrates the PS-containing lipid monolayer more effectively than wild type (Fig. 6), and shows little PS selectivity in vesicle binding and enzymatic action (Table I and Fig. 7). Because the mutations of hydrophobic residues in the C1B domain of PKCδ had essentially no effect on both the *in vitro* and cellular membrane affinity and activity of PKCδ, it is not likely that the role of $Asp^{245}$ is to tether the C1B domain, as proposed for $Asp^{116}$ of the C1A domain. More likely, it would influence the tethering of the C1A domain to the PKC molecule, directly or indirectly. Although further studies are needed to address this issue, one can speculate that the difference between PKCα and PKCδ in terms of the role of the anionic residue in the C1B domain ($Asp^{116}$ of PKCα and $Asp^{245}$ of PKCδ) might derive from the different structural arrangements of C1 and C2 domains and the different properties of their C2 domains. For example, the C2 domain of PKCα has been shown to specifically bind PS (49, 77) and plays a key role in the $Ca^{2+}$-dependent membrane binding of protein (33, 59, 60), whereas that of PKCδ seems to play a direct role in neither PS (or membrane) binding nor PS specificity (see Table I). These differences might also explain why PKCδ requires a higher PS concentration than PKCα for the membrane binding, monolayer penetration, and activation.

Our recent studies on various membrane targeting domains and proteins have shown that the lipid head group specificity and membrane affinity of these proteins govern the destination and efficiency of their subcellular membrane targeting, respectively (33, 49, 78, 79). Specifically, it has been demonstrated that proteins with PS specificity, including the C2 domain of PKCα, are either pre-localized or targeted to the PS-rich cytoplasmic leaflet of the plasma membrane (49). Not taking into account the potential protein-protein interactions (75, 76), PKCδ is expected to translocate to any cell membranes containing DAG, if its membrane targeting is solely driven by C1A-DAG interactions. However, our *in vitro* binding study using cell membrane-mimicking vesicles and our membrane translocation study in HEK293 cells show that the PS specificity of PKCδ plays a decisive role in its subcellular localization. PKCδ preferentially translocates to the plasma membrane when DAG is randomly distributed among cell membranes. More important, this specific targeting can be significantly disrupted by reducing its PS specificity, as seen for E177A and D245A. In conjunction with the good semiquantitative correlation between the *in vitro* membrane affinity of PKCδ mutants and the rate and extent of their cellular membrane translocation (Fig. 8*E*), this also suggests that membrane-protein interactions play a major role in the cellular membrane targeting of PKCδ, at least in HEK293 cells under our experimental conditions. This notion is further supported by the finding that the disruption of cytoskeletal proteins in HEK293 cells did not have any detectable effect on the membrane translocation of PKCδ.

Apparently, our results are at odds with recent reports indicating that PKCδ is specifically targeted to the mitochondria (80, 81) and the nucleus (9–11, 28). It should be noted that these studies were performed under different conditions and typically on longer time scales (*i.e.* >1 h incubation). Under our experimental conditions (*i.e.* OPG or $DiC_8$ activation for <30 min), PKCδ did not induce apoptosis in HEK293 cells and shows no detectable translocation to the mitochondria and the nucleus. However, it should be noted that the C1A domain of PKCδ, as with other C1 domains, would sensitively monitor the spatiotemporal dynamics of DAG and that PKCδ would specifically translocate to the mitochondria if DAG is generated

mainly at the outer mitochondrial membrane under certain physiological conditions. It is also possible that PKCδ is targeted to other organelles via its initial plasma membrane localization, as reported for other proteins (82).

Opposing cellular actions of two novel PKCs, PKCδ and PKCε, have been reported under different conditions (7, 16–18). Although specific cellular adaptor proteins that mediate differential membrane localization and activities of the two PKCs have been reported (16, 75, 83, 84), our present study implies that distinct membrane binding and activation mechanisms of these PKCs might also contribute to their differential cellular actions. Our previous study showed that PKCε has little PS specificity and has generally lower affinity than PKCα for any anionic vesicles (*e.g.* POPC/POPS/DiC$_{18}$ (69:30:1)) (52). Our preliminary study[3] also indicates that neither C1A nor C1B domains of PKCε are conformationally restricted, as is the case with PKCγ (38). PKCδ is similar to PKCε in that both have lower affinity for PS-containing vesicles and lower penetration into PS-containing monolayers than PKCα, presumably because of the lack of $Ca^{2+}$- and membrane-binding C2 domains. Unlike PKCε, however, PKCδ displays clear PS specificity, which should differentially affect their membrane targeting and activation in the cell.

In summary, this study illustrates the mechanism by which a novel PKC, PKCδ, binds model and cell membranes and gets activated in response to DAG. The study provides another example of how structural differences among PKC isoforms cause the differences in membrane binding and activation mechanisms. It also underscores the fact that many PKC isoforms are activated by different mechanisms when activated by DAG and phorbol esters, respectively. The PS specificity of PKCδ, which is likely to derive from the specific unlocking of the tethered C1A domain by PS, causes this PKC to translocate preferentially to the PS-rich plasma membrane, thereby allowing its specific activation in the plasma membrane under certain physiological conditions. In conjunction with our previous mechanistic studies on conventional PKCs, this study provides a basis for further investigation of the molecular mechanisms underlying the subcellular targeting and activation of other novel PKC isoforms.

REFERENCES


1. Newton, A. C. (2001) *Chem. Rev.* **101,** 2353–2364
2. Newton, A. C. (2003) *Methods Mol. Biol.* **233,** 3–7
3. Ono, Y., Fujii, T., Ogita, K., Kikkawa, U., Igarashi, K., and Nishizuka, Y. (1988) *J. Biol. Chem.* **263,** 6927–6932
4. Leibersperger, H., Gschwendt, M., Gernold, M., and Marks, F. (1991) *J. Biol. Chem.* **266,** 14778–14784
5. Wetsel, W. C., Khan, W. A., Merchenthaler, I., Rivera, H., Halpern, A. E., Phung, H. M., Negro-Vilar, A., and Hannun, Y. A. (1992) *J. Cell Biol.* **117,** 121–133
6. Fukumoto, S., Nishizawa, Y., Hosoi, M., Koyama, H., Yamakawa, K., Ohno, S., and Morii, H. (1997) *J. Biol. Chem.* **272,** 13816–13822
7. Mischak, H., Goodnight, J. A., Kolch, W., Martiny-Baron, G., Schaechtle, C., Kazanietz, M. G., Blumberg, P. M., Pierce, J. H., and Mushinski, J. F. (1993) *J. Biol. Chem.* **268,** 6090–6096
8. Watanabe, T., Ono, Y., Taniyama, Y., Hazama, K., Igarashi, K., Ogita, K., Kikkawa, U., and Nishizuka, Y. (1992) *Proc. Natl. Acad. Sci. U. S. A.* **89,** 10159–10163
9. Emoto, Y., Manome, Y., Meinhardt, G., Kisaki, H., Kharbanda, S., Robertson, M., Ghayur, T., Wong, W. W., Kamen, R., and Weichselbaum, R. (1995) *EMBO J.* **14,** 6148–6156
10. Ghayur, T., Hugunin, M., Talanian, R. V., Ratnofsky, S., Quinlan, C., Emoto, Y., Pandey, P., Datta, R., Huang, Y., Kharbanda, S., Allen, H., Kamen, R., Wong, W., and Kufe, D. (1996) *J. Exp. Med.* **184,** 2399–2404
11. Mizuno, K., Noda, K., Araki, T., Imaoka, T., Kobayashi, Y., Akita, Y., Shimonaka, M., Kishi, S., and Ohno, S. (1997) *Eur. J. Biochem.* **250,** 7–18
12. Wang, Q. J., Acs, P., Goodnight, J., Giese, T., Blumberg, P. M., Mischak, H., and Mushinski, J. F. (1997) *J. Biol. Chem.* **272,** 76–82
13. Miyamoto, A., Nakayama, K., Imaki, H., Hirose, S., Jiang, Y., Abe, M., Tsukiyama, T., Nagahama, H., Ohno, S., Hatakeyama, S., and Nakayama, K. I. (2002) *Nature* **416,** 865–869
14. Leitges, M., Gimborn, K., Elis, W., Kalesnikoff, J., Hughes, M. R., Krystal, G., and Huber, M. (2002) *Mol. Cell. Biol.* **22,** 3970–3980
15. Wakino, S., Kintscher, U., Liu, Z., Kim, S., Yin, F., Ohba, M., Kuroki, T., Schonthal, A. H., Hsueh, W. A., and Law, R. E. (2001) *J. Biol. Chem.* **276,** 47650–47657
16. Mackay, K., and Mochly-Rosen, D. (2001) *J. Mol. Cell Cardiol.* **33,** 1301–1307
17. Liu, H., McPherson, B. C., and Yao, Z. (2001) *Am. J. Physiol.* **281,** H404–H410
18. Clarke, H., Ginanni, N., Soler, A. P., and Mullin, J. M. (2000) *Kidney Int.* **58,** 1004–1015
19. Kikkawa, U., Matsuzaki, H., and Yamamoto, T. (2002) *J. Biochem.* (*Tokyo*) **132,** 831–839
20. Newton, A. C. (2003) *Biochem. J.* **370,** 361–371
21. Parekh, D. B., Ziegler, W., and Parker, P. J. (2000) *EMBO J.* **19,** 496–503
22. Chou, M. M., Hou, W., Johnson, J., Graham, L. K., Lee, M. H., Chen, C. S., Newton, A. C., Schaffhausen, B. S., and Toker, A. (1998) *Curr. Biol.* **8,** 1069–1077
23. Dutil, E. M., Toker, A., and Newton, A. C. (1998) *Curr. Biol.* **8,** 1366–1375
24. Keranen, L. M., Dutil, E. M., and Newton, A. C. (1995) *Curr. Biol.* **5,** 1394–1403
25. Konishi, H., Yamauchi, E., Taniguchi, H., Yamamoto, T., Matsuzaki, H., Takemura, Y., Ohmae, K., Kikkawa, U., and Nishizuka, Y. (2001) *Proc. Natl. Acad. Sci. U. S. A.* **98,** 6587–6592
26. Stempka, L., Schnolzer, M., Radke, S., Rincke, G., Marks, F., and Gschwendt, M. (1999) *J. Biol. Chem.* **274,** 8886–8892
27. Stempka, L., Girod, A., Muller, H. J., Rincke, G., Marks, F., Gschwendt, M., and Bossemeyer, D. (1997) *J. Biol. Chem.* **272,** 6805–6811
28. DeVries, T. A., Neville, M. C., and Reyland, M. E. (2002) *EMBO J.* **21,** 6050–6060
29. Kazanietz, M. G. (2002) *Mol. Pharmacol.* **61,** 759–767
30. Ron, D., and Kazanietz, M. G. (1999) *FASEB J.* **13,** 1658–1676
31. Brose, N., and Rosenmund, C. (2002) *J. Cell Sci.* **115,** 4399–4411
32. Yang, C., and Kazanietz, M. G. (2003) *Trends Pharmacol. Sci.* **24,** 602–608
33. Cho, W. (2001) *J. Biol. Chem.* **276,** 32407–32410
34. Nalefski, E. A., and Falke, J. J. (1996) *Protein Sci.* **5,** 2375–2390
35. Rizo, J., and Sudhof, T. C. (1998) *J. Biol. Chem.* **273,** 15879–15882
36. Sutton, R. B., Davletov, B. A., Berghuis, A. M., Sudhof, T. C., and Sprang, S. R. (1995) *Cell* **80,** 929–938
37. Bogi, K., Lorenzo, P. S., Szallasi, Z., Acs, P., Wagner, G. S., and Blumberg, P. M. (1998) *Cancer Res.* **58,** 1423–1428
38. Ananthanarayanan, B., Stahelin, R. V., Digman, M. A., and Cho, W. (2003) *J. Biol. Chem.* **278,** 46886–46894
39. Kates, M. (1986) in *Techniques of Lipidology* (Burdon, R. H., and van Knippenburg, P. H., ed) 2nd Ed., pp. 114–115, Elsevier Science Publishers B. V., Amsterdam
40. Ho, S. N., Hunt, H. D., Horton, R. M., Pullen, J. K., and Pease, L. R. (1989) *Gene* (*Amst.*) **77,** 51–59
41. Cho, W., Digman, M., Ananthanarayanan, B., and Stahelin, R. V. (2003) *Methods Mol. Biol.* **233,** 291–298
42. Bittova, L., Sumandea, M., and Cho, W. (1999) *J. Biol. Chem.* **274,** 9665–9672
43. Cho, W., Bittova, L., and Stahelin, R. V. (2001) *Anal. Biochem.* **296,** 153–161
44. Bittova, L., Stahelin, R. V., and Cho, W. (2001) *J. Biol. Chem.* **276,** 4218–4226
45. Stahelin, R. V., and Cho, W. (2001) *Biochemistry* **40,** 4672–4678
46. Stahelin, R. V., and Cho, W. (2001) *Biochem. J.* **359,** 679–685
47. Myszka, D. G. (1997) *Curr. Opin. Biotechnol.* **8,** 50–57
48. Myszka, D. G. (1999) *J. Mol. Recognit.* **12,** 279–284
49. Stahelin, R. V., Rafter, J. D., Das, S., and Cho, W. (2003) *J. Biol. Chem.* **278,** 12452–12460
50. Newton, A. C. (1993) *Annu. Rev. Biophys. Biomol. Struct.* **22,** 1–25
51. Newton, A. C., and Keranen, L. M. (1994) *Biochemistry* **33,** 6651–6658
52. Medkova, M., and Cho, W. (1998) *Biochemistry* **37,** 4892–4900
53. Kazanietz, M. G., Barchi, J. J., Jr., Omichinski, J. G., and Blumberg, P. M. (1995) *J. Biol. Chem.* **270,** 14679–14684
54. Mozsolits, H., and Aguilar, M. I. (2002) *Biopolymers* **66,** 3–18
55. Mozsolits, H., Thomas, W. G., and Aguilar, M. I. (2003) *J. Pept. Sci.* **9,** 77–89
56. Stahelin, R. V., Long, F., Diraviyam, K., Bruzik, K. S., Murray, D., and Cho, W. (2002) *J. Biol. Chem.* **277,** 26379–26388
57. Stahelin, R. V., Burian, A., Bruzik, K. S., Murray, D., and Cho, W. (2003) *J. Biol. Chem.* **278,** 14469–14479
58. Bazzi, M. D., and Nelsestuen, G. L. (1988) *Biochemistry* **27,** 6776–6783
59. Newton, A. C. (1995) *Curr. Biol.* **5,** 973–976
60. Medkova, M., and Cho, W. (1998) *J. Biol. Chem.* **273,** 17544–17552
61. Ochoa, W. F., Garcia-Garcia, J., Fita, I., Corbalan-Garcia, S., Verdaguer, N., and Gomez-Fernandez, J. C. (2001) *J. Mol. Biol.* **311,** 837–849
62. Pepio, A. M., and Sossin, W. S. (2001) *J. Biol. Chem.* **276,** 3846–3855
63. Pappa, H., Dekker, L. V., Parker, P. J., and McDonald, N. Q. (1998) *Acta Crystallogr. Sect. D Biol. Crystallogr.* **54**, 693–696
64. Pappa, H., Murray-Rust, J., Dekker, L. V., Parker, P. J., and McDonald, N. Q. (1998) *Structure* **6,** 885–894
65. Medkova, M., and Cho, W. (1999) *J. Biol. Chem.* **274,** 19852–19861
66. Zhang, G., Kazanietz, M. G., Blumberg, P. M., and Hurley, J. H. (1995) *Cell* **81,** 917–924
67. Szallasi, Z., Bogi, K., Gohari, S., Biro, T., Acs, P., and Blumberg, P. M. (1996) *J. Biol. Chem.* **271,** 18299–18301
68. Lorenzo, P. S., Bogi, K., Hughes, K. M., Beheshti, M., Bhattacharyya, D., Garfield, S. H., Pettit, G. R., and Blumberg, P. M. (1999) *Cancer Res.* **59,** 6137–6144
69. Wang, Q. J., Bhattacharyya, D., Garfield, S., Nacro, K., Marquez, V. E., and Blumberg, P. M. (1999) *J. Biol. Chem.* **274,** 37233–37239
70. Wang, Q. J., Fang, T. W., Fenick, D., Garfield, S., Bienfait, B., Marquez, V. E., and Blumberg, P. M. (2000) *J. Biol. Chem.* **275,** 12136–12146
71. Wang, Q. J., Fang, T. W., Nacro, K., Marquez, V. E., Wang, S., and Blumberg, P. M. (2001) *J. Biol. Chem.* **276,** 19580–19587
72. Aroca, P., Santos, E., and Kazanietz, M. G. (2000) *FEBS Lett.* **483,** 27–32
73. Irie, K., Oie, K., Nakahara, A., Yanai, Y., Ohigashi, H., Wender, P. A., Fukuda,


[3] R. V. Stahelin and W. Cho, manuscript in preparation.

H., Konishi, H., and Kikkawa, U. (1998) *J. Am. Chem. Soc.* **120,** 9159–9167
74. Slater, S. J., Ho, C., Kelly, M. B., Larkin, J. D., Taddeo, F. J., Yeager, M. D., and Stubbs, C. D. (1996) *J. Biol. Chem.* **271,** 4627–4631
75. Lopez-Lluch, G., Bird, M. M., Canas, B., Godovac-Zimmerman, J., Ridley, A., Segal, A. W., and Dekker, L. V. (2001) *Biochem. J.* **357,** 39–47
76. Song, J. S., Swann, P. G., Szallasi, Z., Blank, U., Blumberg, P. M., and Rivera, J. (1998) *Oncogene* **16,** 3357–3368
77. Verdaguer, N., Corbalan-Garcia, S., Ochoa, W. F., Fita, I., and Gomez-Fernandez, J. C. (1999) *EMBO J.* **18,** 6329–6338
78. Ananthanarayanan, B., Das, S., Rhee, S. G., Murray, D., and Cho, W. (2002) *J. Biol. Chem.* **277,** 3568–3575
79. Kulkarni, S., Das, S., Funk, C. D., Murray, D., and Cho, W. (2002) *J. Biol. Chem.* **277,** 13167–13174
80. Majumder, P. K., Pandey, P., Sun, X., Cheng, K., Datta, R., Saxena, S., Kharbanda, S., and Kufe, D. (2000) *J. Biol. Chem.* **275,** 21793–21796
81. Caruso, M., Maitan, M. A., Bifulco, G., Miele, C., Vigliotta, G., Oriente, F., Formisano, P., and Beguinot, F. (2001) *J. Biol. Chem.* **276,** 45088–45097
82. Matthews, S. A., Iglesias, T., Rozengurt, E., and Cantrell, D. (2000) *EMBO J.* **19,** 2935–2945
83. Mochly-Rosen, D., Henrich, C. J., Cheever, L., Khaner, H., and Simpson, P. C. (1990) *Cell Regul.* **1,** 693–706
84. Mochly-Rosen, D., and Gordon, A. S. (1998) *FASEB J.* **12,** 35–42

# Mechanism of Diacylglycerol-induced Membrane Targeting and Activation of Protein Kinase C δ

Robert V. Stahelin, Michelle A. Digman, Martina Medkova, Bharath Ananthanarayanan, John D. Rafter, Heather R. Melowic and Wonhwa Cho

*J. Biol. Chem. 2004, 279:29501-29512.*
*doi: 10.1074/jbc.M403191200 originally published online April 22, 2004*

---